Retrieval of Surface Temperature and Emissivity From Ground-Based Time-Series Thermal Infrared Data

Yonggang Qian, Ning Wang, Kun Li, Hua Wu, Sibo Duan, Yaokai Liu, Lingling Ma, Caixia Gao, Shi Qiu, Lingli Tang, and Chuanrong Li

***Abstract*—This article addressed the simultaneous retrieval of land surface temperature (LST) and emissivity (LST&E) from the time-series thermal infrared data. On the basis of the assumption that the time-series LSTs can be described by a piecewise linear function, a new method has been proposed to simultaneously retrieve LST&E from atmospherically corrected time-series thermal infrared data using LST linear constraint. A detailed analysis has been performed against various errors, including error introduced by the method assumption, instrument noise, initial emissivity, atmospheric downwelling radiance error, etc. The proposed method from the simulated data is more immune to noise than the existing methods. Even with a noise equivalent delta temperature of 0.5 K, the root-mean-square error of LST is observed to be only 0.13 K, and that of the land surface emissivity (LSE) is 1.8E-3. In addition, our proposed method is simple and efficient and does not encounter the problem of singular values unlike the existing methods. To validate the proposed method, a field experiment from June to September 2017 was conducted for sand target in Baotou site, China. The results show that the samples have an accuracy of LST within 0.87 K and that the mean values of LSE are accurate to 0.01.**

***Index Terms*—Land surface temperature (LST), emissivity, time series, thermal infrared data.**

Manuscript received August 21, 2019; revised November 18, 2019; accepted December 10, 2019. Date of publication January 2, 2020; date of current version February 12, 2020. This work was supported in part by the National Key Research and Development Program of China under Grant 2016YFB0500400, in part by the National Natural Science Foundation of China under Grant 41871221, in part by the Strategic Priority Research Program of the Chinese Academy of Sciences under Grant XDA13030402, and in part by Youth Innovation Promotion Association CAS. *(Corresponding authors: Kun Li; Yaokai Liu.)*

Y. Qian, N. Wang, K. Li, Y. Liu, L. Ma, C. Gao, S. Qiu, L. Tang, and C. Li are with the Key Laboratory of Quantitative Remote Sensing Information Technology, Aerospace Information Research Institute, Chinese Academy of Sciences, Beijing 100094, China (e-mail: qianyg@aoe.ac.cn; wangning@aoe.ac.cn; likun@aoe.ac.cn; liuyk@aoe.ac.cn; llma@aoe.ac.cn; gaocx@aoe.ac.cn; qiushi@aoe.ac.cn; tanglingli@aoe.ac.cn; Lichuanrong@aoe.ac.cn).

H. Wu is with the State Key Laboratory of Resources and Environmental Information System, Institute of Geographical Sciences and Natural Resources Research, Chinese Academy of Sciences, Beijing 100101, China (e-mail: wuhua@igsnrr.ac.cn).

S. Duan is with the Key Laboratory of Agricultural Remote Sensing, Ministry of Agriculture/Institute of Agricultural Resources and Regional Planning, Chinese Academy of Agricultural Sciences, Beijing 100081, China (e-mail: duansibo@163.com).

Digital Object Identifier 10.1109/JSTARS.2019.2959794

I. Introduction

LAND surface temperature (LST) is one of the key parameters in the physics of land surface processes, combining the surface–atmosphere interactions and the energy fluxes between the atmosphere and the ground [1]. LST is required for a wide variety of scientific studies—from climatology to hydrology to ecology and biogeology, such as the energy budget modeling and evapotranspiration modeling, estimating soil moisture, frost detection and forecasting, monitoring the state of the crops [2], studying land and sea breezes, and nocturnal cooling. LST is also a good indicator of the greenhouse effect, and the radiative transfer simulations based on the observed surface temperature data show a positive correlation between the normalized greenhouse effect and the surface temperature [3]. Accurate LSTs would not only help to estimate surface energy and water balances, thermal inertia, and soil moisture [4], [5], it would also enable an analysis of the global surface temperature and its variability within a long period of time.

One key parameter to derive LST is land surface emissivity (LSE). LSE is the ratio of the radiance emitted by an actual land surface at some temperature to the theoretical radiance emitted by a blackbody at the same temperature. It is a measure of a material's ability to absorb and radiate energy. LSE is an intrinsic property of the surface and is almost independent of the temperature under natural conditions [6], e.g., the channel-averaged emissivity in AVHRR channel 3 for coarse sand changes only 0.004 over the temperature range of 240–320 K [7]. LSE can also support more accurate retrievals of atmospheric properties, such as temperature and moisture profiles from multispectral satellite radiance measurements.

Many land surface temperature and emissivity (LST&E) retrieval methods from the remotely sensed multiple thermal infrared data have been proposed [8], [9]. The temperature-emissivity separation methods include the classification-based emissivity retrieval method [10], the reference channel method [11], the emissivity normalization method [12], the spectral ratio method [13], the alpha emissivity method [14] and the physics-based emissivity-temperature decoupling method based on the temperature-independent spectral indices concept [6], the iterative spectrally smooth temperature and emissivity separation (ISSTES) method [15], [16], and the stepwise refining algorithm of temperature and emissivity separation method [17].

LST retrieval algorithms are based on the radiative transfer theory.

In this article, an LST&E retrieval method has been proposed from the ground-based time-series single-band TIR data. This article is organized as follows. Section II describes the theoretical method, including the basic theory and the separation of LST&E. Section III introduces the time-series data measured by thermometers. In Section IV, the sensitivity analysis of the new method with respect to measurement noise and uncertainty of LSE and atmospheric downwelling radiance. The new method is applied to the soil and vegetation areas in Section V, and finally, the conclusion is given.

II. Method

A. Thermal Radiative Transfer Equation

According to the radiative transfer theory, for a cloud-free atmosphere under local thermodynamic equilibrium, the TIR channel radiance L received by the sensor can approximately be written as [18]

$$L(T) = \tau\varepsilon B(T_s) + \tau(1-\varepsilon)L_{\mathrm{atm}\downarrow} + L_{\mathrm{atm}\uparrow} \tag{1}$$

where T is the at-sensor brightness temperature, ε is the LSE, τ is the channel atmospheric transmittance, $B(T_s)$ is Planck's function at T_s, $L_{\mathrm{atm}\uparrow}$ is the upwelling atmospheric channel radiance, and $L_{\mathrm{atm}\downarrow}$ is the channel downward atmospheric radiance, defined as $1/\pi$ times the total downward atmospheric radiance.

It is obvious that the retrieval of LST&E from (1), the atmospheric parameters including τ, $L_{\mathrm{atm}\downarrow}$, and $L_{\mathrm{atm}\uparrow}$ should be removed first. The equation can be written as follows after atmospheric correction:

$$L_g(T_g) = \varepsilon B(T_s) + (1-\varepsilon)L_{\mathrm{atm}\downarrow}. \tag{2}$$

$L_g(T_g)$ is the at-ground channel radiance. T_g is the brightness temperature at the ground level. In this article, to validate the feasibility of the proposed method, the ground-based measurement data are used for analysis in following section.

B. Retrieval of LST and Emissivity From Time-Series Data

For a sensor with N infrared spectral channels, there are N measurements but $N+1$ unknown (N channel emissivities plus one surface temperature). For resolving this ill-posed problem, additional assumptions are necessary to constrain the extra degree of freedom, which has led to different temperature-emissivity separation methods [19], [20]. There are generally two ways to solve this ill-posed problem [21]. In this article, the ill-posed problem is that for a sensor with one infrared channel and N time-series measurement data, there are N measurements but $N+1$ unknown (one channel emissivity plus N time-series temperatures). To solve the ill-posed problem, one could fit the time-series LSTs with a polynomial curve to reduce the number of unknowns. Thus, we assumed that the relationship between the time-series temperature and time can be expressed as a piecewise linear function.

By assuming that there are N time-series TIR data, accordingly, there are N LSTs. As shown in Fig. 1, by dividing the time-series LSTs into M sections, with each section containing C_i LSTs, the whole time-series can be fitted by M lines, such as the red lines shown in Fig. 1. Thus, the time-series LSTs can be expressed by a group of linear equations as

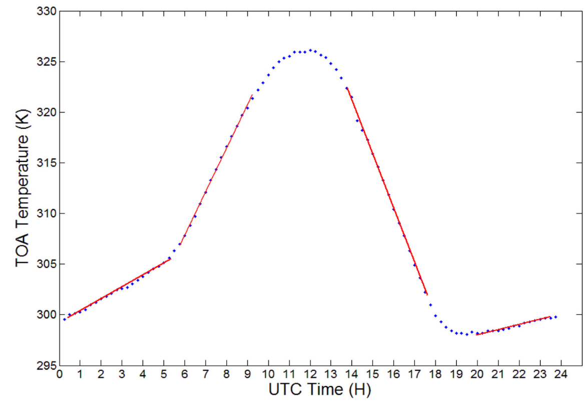

(a) non-cloudy condition

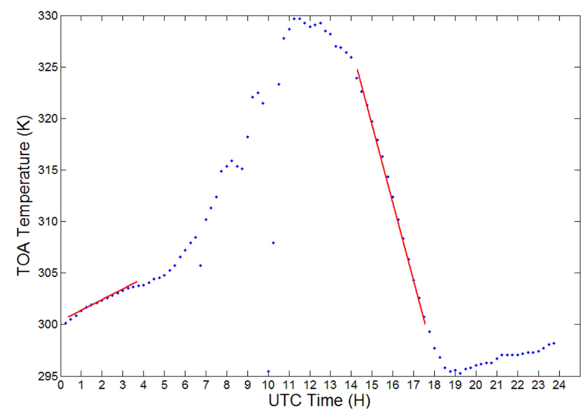

(b) partly cloudy condition

Fig. 1. Sketch map of the piecewise linear time-series temperatures for noncloudy condition. (a) Partly cloudy condition. (b). Blue dot is the actual time-series LST and the red lines are the fitting lines.

$$T_{i,j} = T_{0,j} + k_j \cdot (t_{i,j} - t_{0,j}) \tag{3}$$

where $T_{0,j}$ and k_j are the intercept and slope in j section. $t_{0,j}$ is the beginning time in j section and $t_{i,j}$ is the time at i o'clock in j section. $j = 1, 2, \ldots, M$, $i \in [\Sigma C_i, \Sigma C_{i+1}]$.

Assumed that the atmospheric correction has been performed well. The LST&E retrieval method proposed using the single TIR band with the time-series measurement data can be expressed as the following:

$$\begin{cases} L_g^{t_1}(T^{t_1}) = \varepsilon B(T_s^{t_1}) + (1-\varepsilon)L_{\mathrm{atm}\downarrow}^{t_1} \\ L_g^{t_2}(T^{t_2}) = \varepsilon B(T_s^{t_2}) + (1-\varepsilon)L_{\mathrm{atm}\downarrow}^{t_2} \\ L_g^{t_3}(T^{t_3}) = \varepsilon B(T_s^{t_3}) + (1-\varepsilon)L_{\mathrm{atm}\downarrow}^{t_3} \\ \ldots\ldots \\ L_g^{t_n}(T^{t_n}) = \varepsilon B(T_s^{t_n}) + (1-\varepsilon)L_{\mathrm{atm}\downarrow}^{t_n} \\ T_{i,j} = T_{0,j} + k_j \cdot (t_{i,j} - t_{0,j}) \end{cases} \tag{4}$$

where $t_1, t_2, \ldots, t_n$ is the observation time.

The number of each group time-series LSTs should be larger than or at least equal to three because a linear function fitted with only two times cannot provide additional useful information to meet the aim of reducing the number of unknowns [21].

Obviously, the introduction of the piecewise linear fitting function makes the ill-posed problem to have a deterministic solution because, now, there are N equations to solve $2M + 1$ unknowns (M intercepts, M slopes, and one emissivity). The criterion (cost function) is defined as the sum of the square of the residual errors of the at-ground radiance between the calculated and the actual ones, i.e.

$$f = \sum_{i}^{M} \sum_{j}^{C_i} [\langle L_g(T_{i,j}) \rangle - L_g(T_{i,j})]^2. \quad (5)$$

Next, the least square technique is employed to find the best-fitting temperature and emissivity. To avoid the unordinary cases, a series of error terms, including the least square error of the difference between measured and calculated at-sensor radiances across the spectral range, limit temperature range to a range of temperature to avoid retrieval of high temperatures and low emissivities, "penalty" function, etc., are given in the ARTEMISS algorithm. The error function helps to avoid solutions where the retrieved emissivities are close to zero and have very large temperatures.

III. Data

A. Time-Series Data Simulated From MODTRAN

A simulation dataset is used with different atmospheres and land surface conditions from MODTRAN 5.0. Six MODTRAN standard atmospheric profiles of temperature, moisture, and ozone have been used, covering a wide range of bottom atmospheric temperature and total perceptible water. Meanwhile, 150 atmospheric profiles with the bottom atmospheric temperature varying between 220 and 320 K and total precipitable water (TPW) with relative humidity at any layer smaller than 90% (see Fig. 2) were extracted from TIGR atmospheric profiles [22]. Emissivity spectra of several representative surface materials, including soil, vegetation, water, and ice, were chosen from the ASTER spectral library [23]. Five subranges of the atmosphere water vapor content (WVC): [0–1.25], [1.25–2.25], [2.25–3.25], [3.25–4.25], and [4.25–5.5] g/cm^2 are used.

B. Time-Series Data Measured From Soil Area

To evaluate the performance of the method, a comprehensive field campaign was carried out at the Baotou site in September, 2017. The Baotou site (see Fig. 3) is located in Urad Qianqi, Inner Mongolia, in northern China at a latitude of 40.85°N and a longitude of 109.6°E. The land covers in Baotou site included cropland, herbaceous land, shrubland, grassland, sparse vegetation, urban areas, sand, and water body. In this article, its temperature measured for sands was used to validate the retrieval results by using our proposed method. The SI-111 thermometers were distributed within the sand area covered about 1 km^2 and deployed at nadir to capture the natural variability of the ground radiometric temperature, and the temporal sampling interval is

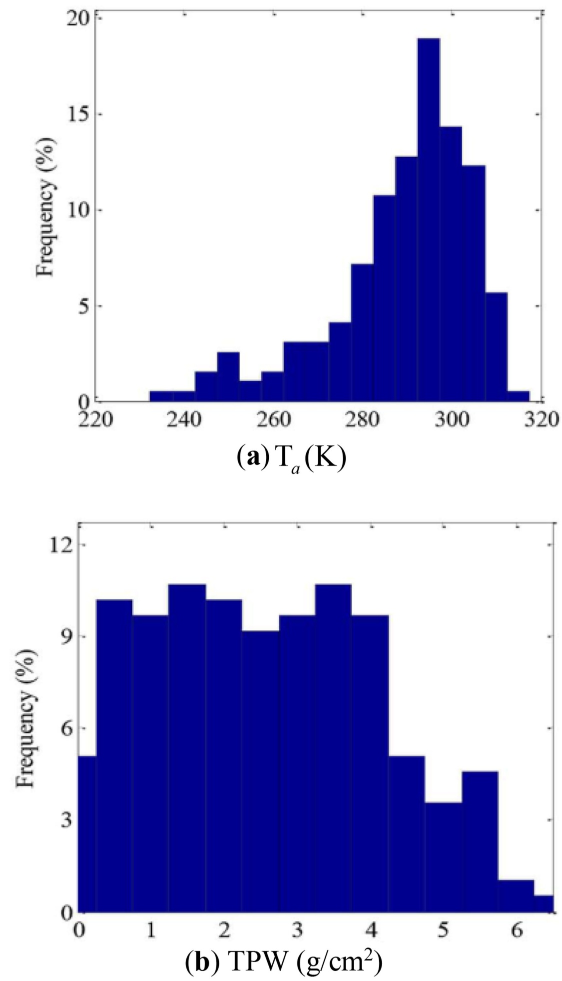

Fig. 2. Histogram of selected atmospheric quantities. (a) Bottom atmospheric temperature. (b) TPW of profiles.

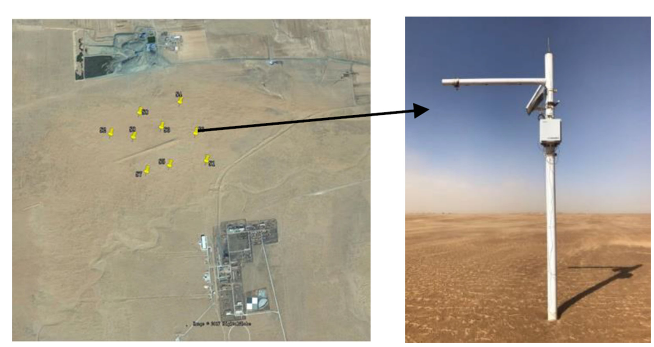

Fig. 3. SI-111 thermometers in the Baotou site.

per minute. Then the continuous LST measurements are used to retrieve the LST&E. The SI-111 thermometer is the spectral range of 8–12 μm and field-of-view (FOV) of 44°.

The radiometric temperatures were measured by the SI-111 thermometers from June to September, 2017. These data will be used for validation of the proposed method. To obtain the actual sand temperature from the field-measured time series data, the environmental downwelling radiance is necessary.

The Baotou site includes the SI-111 radiometers that one vertically measured the surface properties from a 4 m height and the other measured the atmospheric downwelling radiance at an approximately 55° zenith angle [23], [27]. The sampling frequency of the radiometers and the SI-111 radiometers is 1 min. For the SI-111 radiometer measurements, the LST was calculated using the following equation [24], [25]

$$T_s = B^{-1}\left(\frac{L(T) - (1-\varepsilon)\cdot L_{\downarrow}}{\varepsilon}\right) \tag{6}$$

where B is the Planck function, T_s is the surface temperature, ε is the surface emissivity, and $L_{\downarrow}$ is the atmospheric downwelling radiance.

Emissivity measurements were performed using the 102 F Fourier transform infrared spectroradiometer with the spectrum covered from 2 to 16 μm, the spectral resolution of 4 cm^{-1}, and FOV of 4.8°. Then, the spectral emissivity was retrieved using the ISSTES algorithm. Finally, an emissivity value of the SI-111 channel was obtained using the spectral response function [26].

The accuracy of the method is characterized by the root-mean-square errors (RMSEs) of the temperature and the rms of the relative emissivity errors

$$\mathrm{RMSE}_{\mathrm{LST}} = \sqrt{\frac{\sum_{i=1}^{M}\left(\mathrm{LST}_{\mathrm{ret}} - \mathrm{LST}_{\mathrm{true}}\right)^2}{M-1}} \tag{7a}$$

$$\mathrm{RMSE}_{\mathrm{LSE}} = \sqrt{\frac{\sum_{i=1}^{M}\left(\mathrm{LSE}_{\mathrm{ret}} - \mathrm{LSE}_{\mathrm{true}}\right)^2}{M-1}} \tag{7b}$$

where $\mathrm{LST}_{\mathrm{ret}}$ and $\mathrm{LST}_{\mathrm{true}}$ are the retrieved and true temperatures, respectively. $\mathrm{LSE}_{\mathrm{ret}}$ and $\mathrm{LSE}_{\mathrm{true}}$ are the retrieved and true emissivities, respectively. M is the total number of measurements. Therefore, the following results will exhibit the performance of the proposed method.

IV. Results and Analysis

A. *Sensitivity Analysis*

The accuracy of this method is also influenced by the uncertainty of instrument noise, the uncertainty of initial emissivity, and the error of the atmospheric downwelling radiance. A sensitive analysis of the proposed method was, thus, performed with respect to the uncertainty of these parameters using the simulated data from MODTRAN 5.0.

1) Effect of Instrument Noise: The noise equivalent delta temperature (NEΔT) of the TIR sensor with different levels of instrument noise is used to analyze. To analyze the effect of the instrument noise on LST&E retrieval, a Gaussian-distribution noise with a mean of 0 K and a standard deviation of NEΔT = 0.1, 0.2, 0.3, 0.4, and 0.5 K was added to the at-ground brightness temperatures. LST&E with the noised at-ground brightness temperatures was estimated, and the RMSEs of LST&E are calculated. The relative error is shown in Fig. 4 between the LSTs retrieved from the non-noise/noise added brightness temperatures.

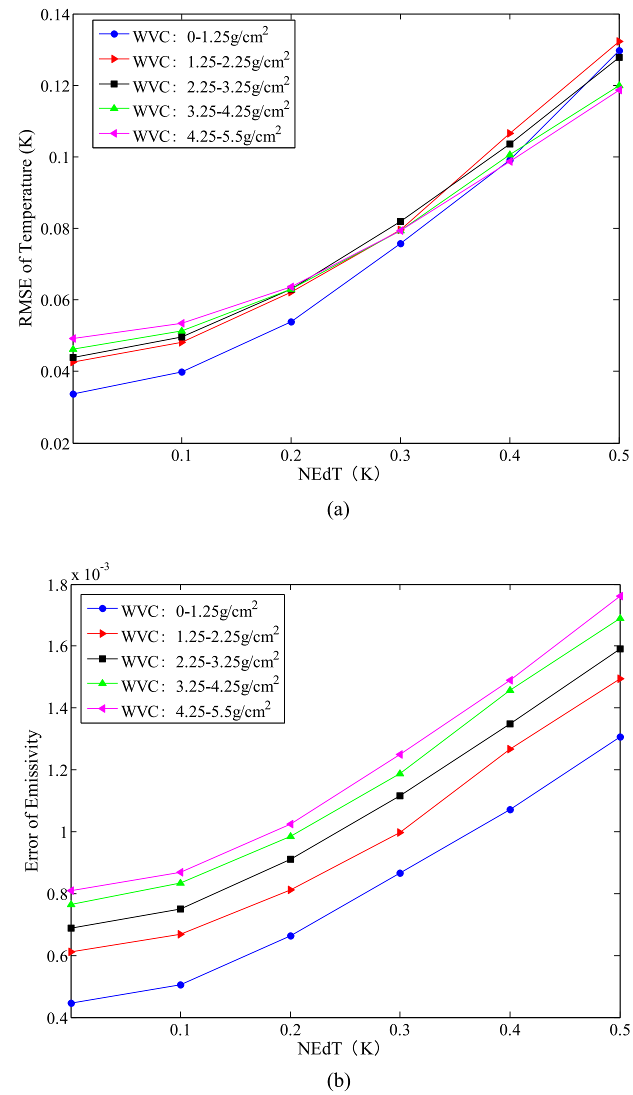

Fig. 4. RMSEs of LST&E caused by instrument noises. (a) LSE of temperature. (b) RMSE of emissivity.

The RMSEs of LST&E are increasing with the increasing NEΔT; meanwhile the RMSEs of LST&E are also increasing with the increasing WVC. It can be seen that the error is relatively small. Even if the NEΔT is up to 0.5 K, the largest RMSEs of LST&E are 0.13 K and 1.8E-3. It is obvious that the errors of the LST&E caused by the NEΔT are very slight.

2) Effect of Initial Emissivity: Initial emissivity is closely related to the LST&E retrieval. To investigate the method's sensitivity to initial emissivity, 0.005, 0.01, 0.015, and 0.02 uncertainties of the initial emissivity of the TIR channel were added in the retrieval of LST using the new method, respectively. In addition, the 0.2 K random noises are added to the at-ground brightness temperatures. The LST&E were retrieved under the five subranges of atmospheric WVCs (see Fig. 5).

The RMSEs of the retrieved LST&E are generally better than 0.6 K and 0.01 under the condition of the 0.01 uncertainty of LSE, respectively. Meanwhile, the RMSEs of the retrieved

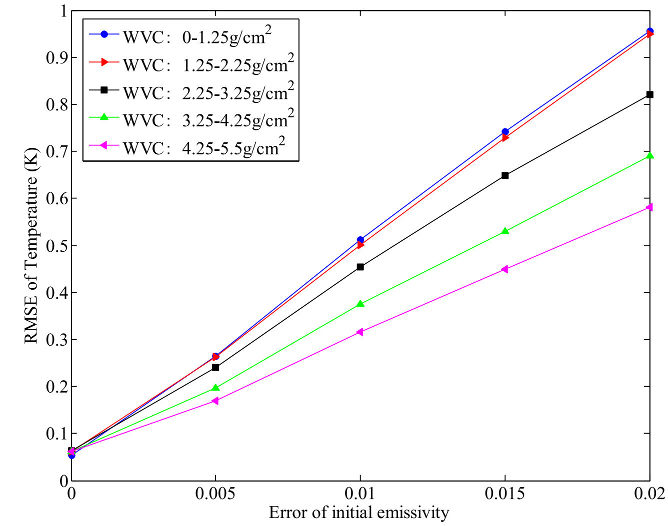

(a)

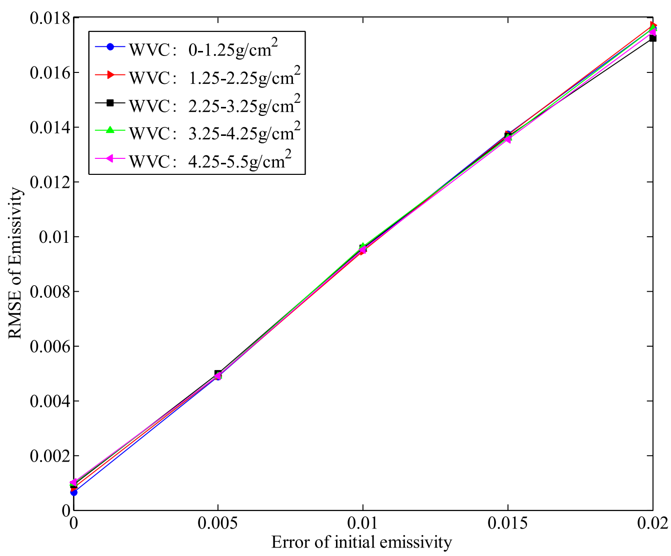

(b)

Fig. 5. RMSEs of LST&E caused by emissivity uncertainty. (a) RMSE of temperature. (b) RMSE of emissivity.

LST&E are better than 1.0 K and 0.018 for all the WVC subranges, when the initial emissivity error is 0.02. It should be noted that the RMSE of LST will be increasing with the decreasing of WVC, while there are no significant influences for emissivity for each WVC subranges.

3) Effect of Initial Atmospheric Downwelling Radiance: The accuracy of LST&E retrieval is influenced significantly by the error of the atmospheric parameters. As well known, the error of the initial atmospheric downwelling radiance will lead to the inaccuracy of at-surface radiance. Consequently, the inaccuracy will affect the retrieval accuracy of LST&E. Thus, to investigate the effects of uncertainties, 5%, 10%, 15%, and 20% uncertainties of atmospheric downwelling radiance are considered, respectively. In addition, the 0.2 K random noises are added to the at-ground brightness temperatures. Then, the error-effected at-ground brightness temperatures are used to estimate the LST&E.

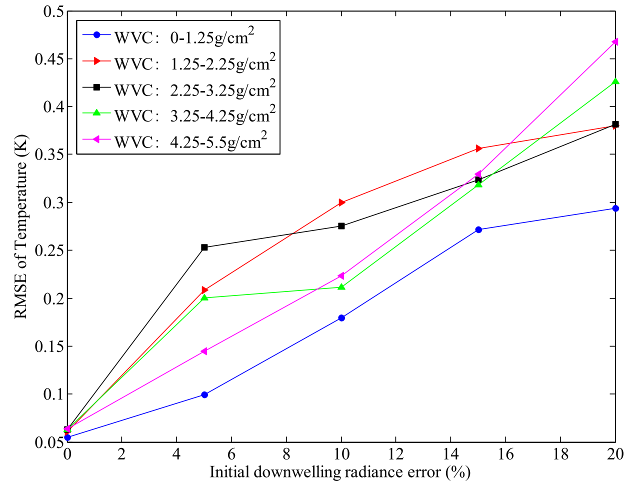

(a)

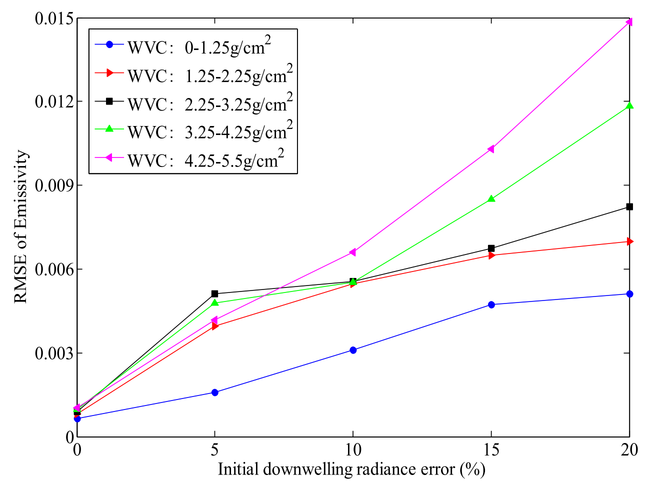

(b)

Fig. 6. RMSEs of LST&E caused by initial atmospheric downwelling radiance. (a) RMSE of temperature. (b) RMSE of emissivity.

The RMSEs of the retrieved LST&E will be increasing with the increase of the initial error of atmospheric downwelling radiance and WVC (see Fig. 6). The RMSEs of the LST&E retrieval results are better than 0.45 K and 0.015 for all WVC subranges under the condition of the 20% uncertainty of initial atmospheric downwelling radiance, respectively. Meanwhile, when the uncertainty of initial atmospheric downwelling radiance is 10%, the RMSEs of the retrieved LST&E are better than 0.3 K and 0.007 for all WVC subranges, respectively. It is obvious that the effect of initial atmospheric downwelling radiance is slight on the errors of the retrieved LST&E.

B. Application to Ground Measured Time-Series Thermal Infrared Data

To evaluate the performance of the proposed method, the time-series thermal infrared data measured by the SI-111 thermometer in Baotou site in 2017 are used. The time range is from

TABLE I
TEMPERATURE AND EMISSIVITY INVERSION RESULTS FROM JUNE TO SEPTEMBER 2017

Month	Item	Bias	RMSE
June	Temperature	-0.09 K	0.76 K
	Emissivity	0.004	0.014
July	Temperature	-0.12 K	0.58 K
	Emissivity	0.007	0.0135
August	Temperature	-0.033K	0.594K
	Emissivity	0.0037	0.0119
September	Temperature	-0.01 K	0.472K
	Emissivity	0.0015	0.0076

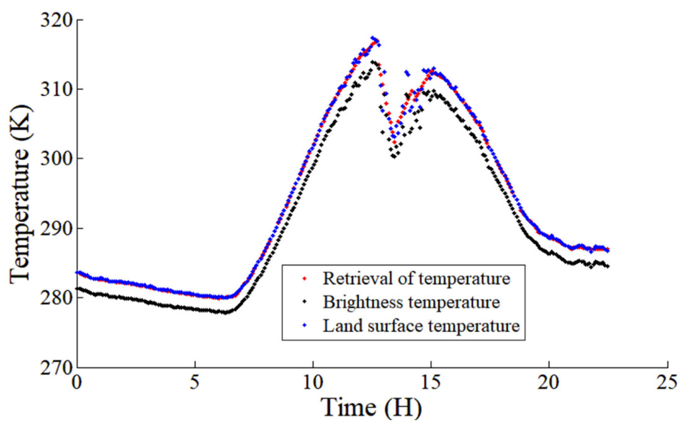

(a)

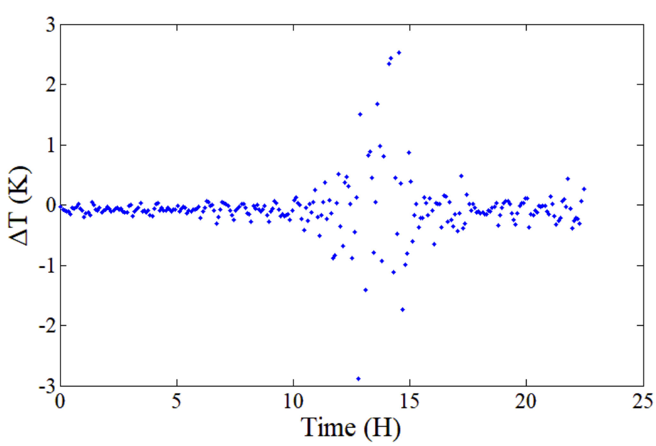

(b)

Fig. 7. Results estimated by the proposed method on 6 September, 2017. (a) The temperature inversion result. (b) The error of temperature.

1 June to 30 September, 2017. The temperature and emissivity are estimated by the proposed method. The bias and RMSE of temperature and emissivity are calculated.

Table I gives the monthly statistics of temperature and emissivity inversion results for June, July, August, and September, 2017. It can be seen that the bias of temperature is about -0.1 K and the bias of emissivity is less than 0.007 for every month.

Figs. 7–9 are the detail results for a single day. The results show that the RMSE of temperature inversion is less than 0.5 K.

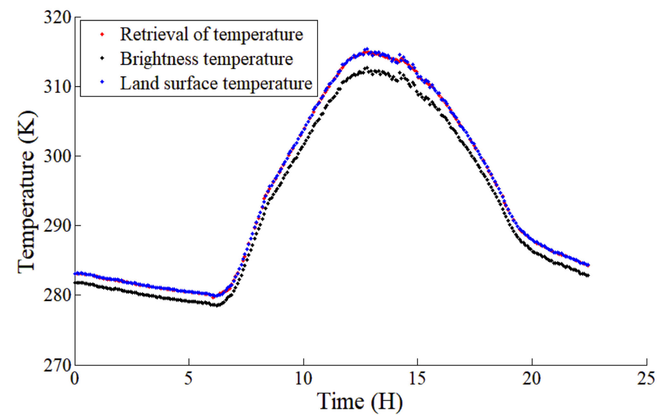

(a)

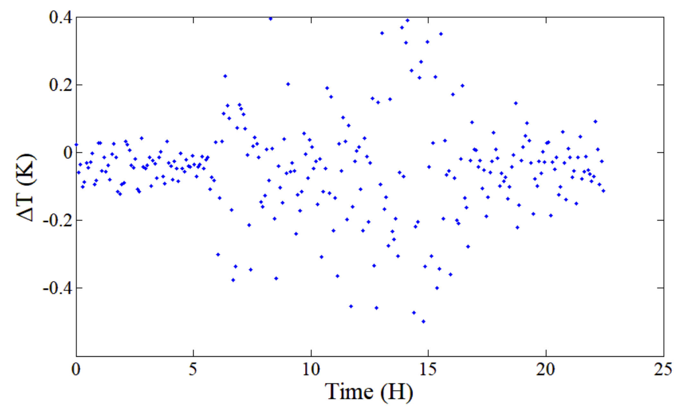

(b)

Fig. 8. Results estimated by the proposed method on 8 September, 2017. (a) The temperature inversion result. (b) The error of temperature.

In addition, it can be seen from the graphs that although the cloud exists in some time periods, it does not affect the overall temperature inversion results. From the error graphs, it can be seen that the temperature inversion error in the cloudy time period is much higher, even to the error of 3 K. The time of high error of temperature inversion almost occurs at noon.

Furthermore, to obtain the more detailed LST inversion results, three time segments, i.e., the morning (local time 0:00–12:00), the noon (local time 12:00–15:00), and the afternoon (local time 15:00–24:00), are used for the analysis separately. Table II is temperature inversion results in different time segment from June to September, 2017. The biases and RMSEs are -0.075 K and 0.753 K, respectively, for all days. The biases of the retrieved LST are underestimated for three time segments. The error of the retrieved LST in the morning and afternoon is close for every month. For the results in the noon, the biases of the LST were also larger than those of the LST in the morning and the afternoon, with bias of -0.1 K for noon, 0.049 K for the morning, and 0.074 K for the afternoon; and the RMSEs are 1.14 K for the noon, 0.53 K for the morning, and 0.59 K for the afternoon. The reason for the largest error in noon is that there are more clouds at noon. In addition, the applicability of the method at noon also needs to be further improved. Because the

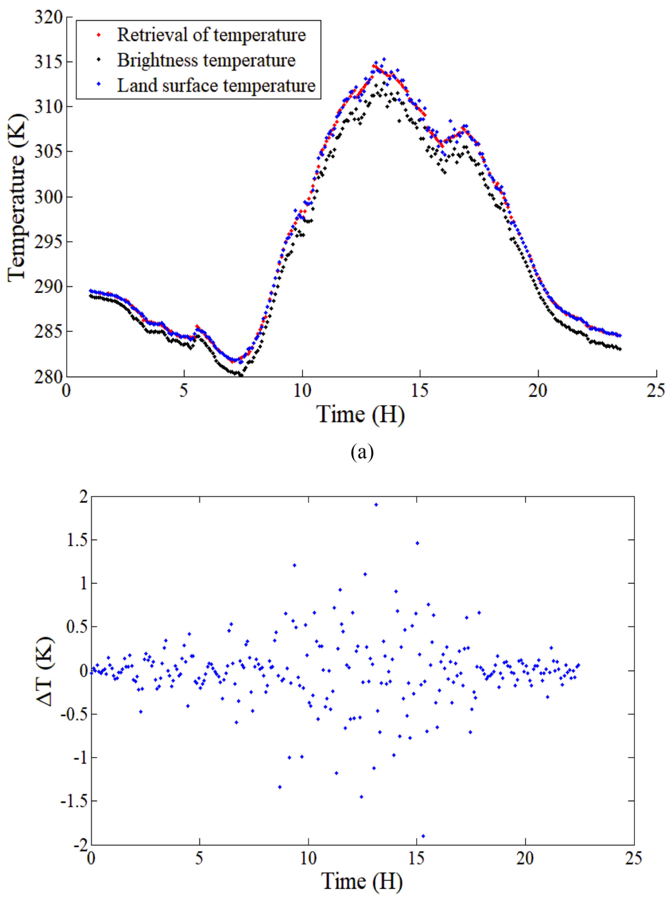

Fig. 9. Results estimated by the proposed method on 9 September, 2017. (a) The temperature inversion result. (b) The error of temperature.

TABLE II
TEMPERATURE INVERSION RESULTS IN DIFFERENT TIME SEGMENT FROM JUNE TO SEPTEMBER 2017

Month	Time	Bias	RMSE
June	0:00-12:00	-0.0817	0.6744
	12:00-15:00	-0.1212	1.3747
	15:00-24:00	-0.0975	0.7505
July	0:00-12:00	-0.098	0.5043
	12:00-15:00	-0.2055	1.1007
	15:00-24:00	-0.1278	0.5690
October	0:00-12:00	-0.018	0.533
	12:00-15:00	-0.059	1.16
	15:00-24:00	-0.047	0.6584
September	0:00-12:00	-1.6e-4	0.41
	12:00-15:00	-0.023	0.921
	15:00-24:00	-0.024	0.384

temperature variation in the daytime shows the cosine function, especially at noon, however, the piecewise linear assumption to fit the time series temperature in the method. It should be noted that the largest error occurred in June because there are more rainfall and dust in this season and the measured data are affected by these factors.

V. CONCLUSION

In this article, a new method for LST and emissivity retrieval from the thermal infrared time series data is proposed. In this method, we assumed that the time series temperature can be depicted by some piecewise linear functions. In this article, the single-band TIR data are used for retrieval. However, the proposed method can be fit for single-band data or multiband data. The time series temperatures of sand are used to analyze the accuracy of the method.

A detailed analysis has been performed against various errors, including error introduced by the method assumption, instrument noise, initial emissivity, atmospheric downwelling radiance error, etc. As for the impact of the atmosphere, the results show that our proposed method performs well with the uncertainty of the atmospheric downwelling radiance but suffers from the inaccuracy of the atmospheric upwelling radiance, which implies that an accurate atmospheric correction is still needed to convert the radiance measured at the satellite level to the at-ground radiance. The proposed method from the simulated data is more noise immune than the existing methods. Even with a NEΔT of 0.5 K, the RMSE of LST is observed to be only 0.13 K and that of LSE is 1.8E-3. In addition, our proposed method is simple and efficient and does not encounter the problem of singular values unlike the existing methods.

The result shows that the LST&Es estimated by this method with the RMSEs are approximately 0.87 K and 0.0097 using the time-series thermal infrared data measured by SI-111 in Baotou site, China. Furthermore, the detailed LST inversion results according to the three time-segments, i.e., the morning, the noon, and the afternoon, are used for analysis separately. The largest error in the noon with LST RMSE of 1.14 K is shown, and the results in the morning and afternoon with LST RMSE 0.53 K and 0.59 K of are similar. Meanwhile, the LST error in June is largest because there are more rainfall and dust in this season and the measured data are affected by many factors. From this study, although the method has already been proposed, it can also be seen that it is necessary to do more work to accurately acquire LST/LSE from remotely sensed thermal infrared time series data.

REFERENCES

[1] P. J. Sellers, F. G. Hall, G. Asrar, D. E. Strebel, and R. E. Murphy, "The first ISLSCP field experiment (FIFE)," *Bull. Amer. Meteorol. Soc.*, vol. 69, pp. 22–27, 1988.

[2] V. Caselles and J. A. Sobrino, "Determination of frosts in orange groves from NOAA-9 AVHRR data," *Remote Sens. Environ.*, vol. 29, pp. 135–146, 1989.

[3] A. Sinha, "Relative influence of lapse rate and water vapor on the greenhouse effect," *J. Geophysical Res.*, vol. 100, pp. 5095–5103, 1995.

[4] J. A. Sobrino and M. Romaguera, "Land surface temperature retrieval from MSG1-SEVIRI data," *Remote Sens. Environ.*, vol. 92, pp. 247–254, 2004.

[5] J. A. Sobrino and J. C. Jiménez-Muñoz, "Minimum configuration of thermal infrared bands for land surface temperature and emissivity estimation in the context of potential future missions," *Remote Sens. Environ.*, vol. 148, pp. 158–167, 2014.
[6] F. Becker and Z.-L. Li, "Temperature independent spectral indices in thermal infrared bands," *Remote Sens. Environ.*, vol. 32, pp. 17–33, 1990.
[7] Z. Wan and J. Dozier, "A generalized split-window algorithm for retrieving land-surface temperature from space," *IEEE Trans. Geosci. Remote Sens.*, vol. 34, no. 4, pp. 892–905, Jul. 1996.
[8] Z.-L. Li *et al.*, "Land surface emissivity retrieval from satellite data," *Int. J. Remote Sens.*, vol. 34, pp. 3084–3127, 2013.
[9] Z.-L. Li *et al.*, "Satellite-derived land surface temperature: Current status and perspectives," *Remote Sens. Environ.*, vol. 131, pp. 14–37, 2013.
[10] W. C. Snyder, Z. Wan, Y. Zhang, and Y.-Z. Feng, "Classification-based emissivity for land surface temperature measurement from space," *Int. J. Remote Sens.*, vol. 19, no. 14, pp. 2753–2774, 1998.
[11] A. B. Kahle and R. E. Alley, "Separation of temperature and emittance in remotely sensed radiance measurements," *Remote Sens. Environ.*, vol. 42, pp. 107–111, 1992.
[12] A. Gillespie, S. Rokugawa, T. Matsunaga, J. S. Cothern, S. Hook, and A. B. Kahle, "A temperature and emissivity separation algorithm for advanced spaceborne thermal emission and reflection radiometer (ASTER) images," *IEEE Trans. Geosci. Remote Sens.*, vol. 36, no. 4, pp. 1113–1126, Jul. 1998.
[13] K. Watson, "Spectral ratio method for measuring emissivity," *Remote Sens. Environ.*, vol. 42, pp. 113–116, 1992.
[14] P. S. Kealy and A. R. Gabell, "Estimation of emissivity and temperature using alpha coefficients," in *Proc. 2nd TIMS Workshop*, Pasadena, CA, USA, 1990, pp. 11–15.
[15] C. C. Borel, "ARTEMISS—An algorithm to retrieve temperature and emissivity from hyper-spectral thermal image data," in *Proc. 28th Annu. GOMACTech Conf. Hyperspectral Imag. Session*, Tampa, FL, USA, Mar. 31/Apr. 3, 2003, pp. 1–4.
[16] C. Borel, "Error analysis for a temperature and emissivity retrieval algorithm for hyperspectral imaging data," *Int. J. Remote Sens.*, vol. 29, pp. 5029–5045, 2008.
[17] J. Cheng, S. Liang, J. Wang, and X. Li, "A stepwise refining algorithm of temperature and emissivity separation for hyperspectral thermal infrared data," *IEEE Trans. Geosci. Remote Sens.*, vol. 48, no. 3, pp. 1588–1597, Mar. 2010.
[18] Z.-L. Li, F. Becker, M. P. Stoll, and Z. M. Wan, "Evaluation of six methods for extracting relative emissivity spectra from thermal infrared images," *Remote Sens. Environ.*, vol. 69, pp. 197–214, 1999.
[19] G.-M. Jiang, Z.-L. Li, and F. Nerry, "Land surface emissivity retrieval from combined mid-infrared and thermal infrared data of MSG-SEVIRI," *Remote Sens. Environ.*, vol. 105, pp. 326–340, 2006.
[20] N. Acito, M. Diani, and G. Corsini, "Subspace-based temperature and emissivity separation algorithms in LWIR hyperspectral data," *IEEE Trans. Geosci. Remote Sens.*, vol. 57, no. 3, pp. 1523–1537, Mar. 2019.
[21] N. Wang, H. Wu, F. Nerry, C. Li, and Z.-L. Li, "Temperature and emissivity retrievals from hyperspectral thermal infrared data using linear spectral emissivity constraint," *IEEE Trans. Geosci. Remote Sens.*, vol. 49, no. 4, pp. 1291–1303, Apr. 2011.
[22] H. Wu, L. Ni, N. Wang, Y. Qian, B.-H. Tang, and Z.-L. Li, "Estimation of atmospheric profiles from hyperspectral infrared IASI sensor," *IEEE J. Sel. Topics Appl. Earth Observ. Remote Sens.*, vol. 6, no. 3, pp. 1485–1494, Jun. 2013.
[23] B.-H. Tang, K. Shao, Z.-L. Li, H. Wu, F. Nerry, and G. Zhou, "Estimation and validation of land surface temperatures from Chinese second-generation polar-orbit FY-3A VIRR data," *Remote Sens.*, vol. 7, pp. 3250–3273, 2015.
[24] Y. Qian *et al.*, "Evaluation of temperature and emissivity retrieval using spectral smoothness method for low-emissivity materials," *IEEE J. Sel. Topics Appl. Earth Observ. Remote Sens.*, vol. 9, no. 9, pp. 4307–4315, Sep. 2016.
[25] Y. G. Qian *et al.*, "Land surface temperature retrieved from airborne multispectral scanner mid-infrared and thermal-infrared data," *Opt. Express*, vol. 24, no. 2, pp. A257–A269, 2016.
[26] E. Zhao, Y. Qian, C. Gao, H. Huo, X. Jiang, and X. Kong, "Land surface temperature retrieval using airborne hyperspectral scanner daytime mid-infrared data," *Remote Sens.*, vol. 6, pp. 12667–12685, 2014.
[27] J.-M. Chen and R.-H. Zhang, "Studies on the measurement of crop emissivity and sky temperature," *Agricultural Forest meteorol.*, vol. 49, pp. 23–34, 1989.

Yonggang Qian received the B.S. degree in applied mathematics from Yantai University, Yantai, China, in 2003, the M.S. degree in geographical information system from the Taiyuan University of Technology, Taiyuan, China, in 2006, and the Ph.D. degree in cartography and geographical information system from Beijing Normal University, Beijing, China, in 2009.

He was a Postdoctor in cartography and geographical information system with the Institute of Geographic Sciences and Natural Resources Research, Chinese Academy of Sciences, Beijing, during 2009–2011.

He is currently a Professor with Aerospace Information Research Institute, Chinese Academy of Sciences, Beijing, China. His research mainly includes the retrieval and validation of surface temperature and emissivity from remotely sensed data.

Ning Wang received the B.S. and M.S. degrees in geophysical science and cartography and geographic information system from Beijing Normal University, Beijing, China, in 2004 and 2007, respectively, and the Ph.D. degree in cartography and geographical information system from the Institute of Geographic Sciences and Natural Resources Research, Chinese Academy of Sciences, Beijing, China, in 2011.

He is currently a Professor with the Aerospace Information Research Institute, Chinese Academy of Sciences. His research interests include thermal infrared remote sensing and hyperspectral remote sensing.

Kun Li received the B.E. degree in remote sensing science and technology from Wuhan University, Wuhan, China, in 2015, and the M.E. degree in electronics and communication engineering from the University of Chinese Academy of Sciences, Beijing, China, in 2018.

He is currently a Research Assistant with Aerospace Information Research Institute, Chinese Academy of Sciences, Beijing, China. His research mainly includes the retrieval and validation of surface temperature and emissivity from remotely sensed data and the directionality of thermal radiance.

Hua Wu received the B.S. degree in photogrammetric engineering and remote sensing from Wuhan University, Wuhan, China, in 2003, the M.S. degree in cartography and geographical information system from Beijing Normal University, Beijing, China, in 2006, and the Ph.D. degree in cartography and geographical information system from the Institute of Geographic Sciences and Natural Resources Research, Chinese Academy of Sciences, Beijing, China, in 2010.

He is currently a Professor with the Institute of Geographic Sciences and Natural Resources Research, Chinese Academy of Sciences. His research mainly includes the retrieval and validation of surface temperature and emissivities and scaling of remotely sensed products.

Sibo Duan received the Ph.D. degree in cartography and geographical information system from the Institute of Geographic Sciences and Natural Resources Research, Chinese Academy of Sciences, Beijing, China, in 2014.

He is currently an Associate Professor with the Institute of Agricultural Resources and Regional Planning, Chinese Academy of Agricultural Sciences, Beijing, China. His current research interests include the retrieval and validation of land surface temperature.

Yaokai Liu received the M.S. degree in cartography and geographical information system from Beijing Normal University, Beijing, China, in 2011, and the Ph.D. degree in signal and information processing from the University of Chinese Academy of Sciences, Beijing, China, in 2018.

He is currently an Associate Researcher with the Aerospace Information Research Institute, Chinese Academy of Sciences, Beijing, China. His research interests focus on field campaigns of remote sensing, hyperspectral data processing and analysis, retrieval of vegetation fractional cover, aerosol optical thickness, and land surface reflectance from remote sensing data.

Lingling Ma received the M.S. and Ph.D. degrees in geography and geographical information system from the Chinese Academy of Sciences, Beijing, China, in 2005 and 2008, respectively.

She is currently a Professor with Aerospace Information Research Institute, Chinese Academy of Sciences, Beijing, China. Her research interests include calibration and validation techniques of remote sensing data and products and inflight performance assessment of optical sensors.

Caixia Gao received the B.S. degree in electronics and information engineering from the Xi'an University of Posts and Telecommunications, Xi'an, China, in 2006, the M.S. degree in computer science from the Academy of Opto-Electronics, Chinese Academy of Sciences, Beijing, China, in 2009, and the Ph.D. degree in cartography and geography information system from the University of Chinese Academy of Sciences, Beijing, China, in 2012.

She is currently an Associate Professor with the Aerospace Information Research Institute, Chinese Academy of Sciences, Beijing, China. Her research interests include the retrieval and validation of surface temperature and emissivities and the intercalibration of satellite sensors.

Shi Qiu received the B.E. degree in engineering from the Huazhong University of Science and Technology, Wuhan, China, in 2007, and the Ph.D. degree in physical education from the University of Strasbourg, Strasbourg, France, in June 2013.

She is currently an Associate Professor with the Aerospace Information Research Institute, Chinese Academy of Sciences, Beijing, China. Her research interests mainly include the retrieval and validation of surface temperature and emissivity from remotely sensed data.

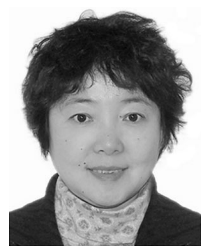

Lingli Tang received the master's degree in image processing from the University of Science and technology of China, in 1980, and the M.S. degree in cartography and geographical information system from ITC, Netherlands, in 1990.

From 1996 to 2006, she was the Director of Data Processing Department, Remote Sensing Satellite Ground Station, Chinese Academy of Sciences (CAS). Since 2006, she has been the Director of Earth Observation Technology Application Department, Academy of Opto-Electronics (nowadays, named as Aerospace Information Research Institute), CAS. Her main expertise fields are in remote sensing satellite ground systems and algorithms of remote sensing image processing.

Chuanrong Li received the master's degree in flight mechanics from the University of Science and technology of China, in 1985.

From 1987 to 2003, he was a Research Scientist with the Remote Sensing Satellite Ground Station, Chinese Academy of Sciences (CAS). He had a postgraduate study experiment from ITC from 1988 to 1990, and has been a Senior Visiting Scholar with CCRS from 1994 to 1995. Since 2003, he has been with the Academy of Opto-Electronics (nowadays, named Aerospace Information Research Institute), CAS, as a Vice President and Research Scientist. He has also been the Co-Chair of the China expert team of COPUOS. He has authored or coauthored more than 50 papers. His main expertise fields are in remote sensing satellite ground systems and algorithms of remote sensing image processing.

Mr. Li was a recipient of the National Scientific and Technological Advancement Award of China in 2003.